

Cathodic Electrodeposition of Chalcogenide Thin Films Cu_4SnS_4 for Solar Cells

Anuar Kassim^{1*}, Ho Soon Min¹, Tan Wee Tee¹, Atan Sharif¹,
Zulkefly Kuang¹, Md. Jelas Haron¹ and Saravanan Nagalingam²

¹Department of Chemistry, Faculty of Science, Universiti Putra Malaysia, 43400 Serdang, Selangor, Malaysia

²Department of Bioscience and Chemistry, Faculty of Engineering and Science, Universiti Tunku Abdul Rahman, 53300 Kuala Lumpur, Malaysia

*Corresponding author. E-mail: anuar@fsas.upm.edu.my

ABSTRACT

Copper tin sulfide thin films were electrodeposited on the indium tin oxide glass substrate in a bath containing CuSO_4 , $\text{SnCl}_2 \cdot 2\text{H}_2\text{O}$ and $\text{Na}_2\text{S}_2\text{O}_3 \cdot 5\text{H}_2\text{O}$ at pH 1 and temperature 25°C. The cyclic voltammetry of the film formation was studied in a potential range of 1000 mV to -1000 mV versus Ag/AgCl. Influence of different deposition potentials on the surface morphology and films structure of Cu_4SnS_4 films was investigated by atomic force microscopy and X-ray diffraction, respectively. The X-ray diffraction data showed the intensity of major peaks at $2\theta = 30.2^\circ$ which belonged to (221) plane of Cu_4SnS_4 . The atomic force microscopy images indicated that the electrodeposited films were smooth, compact and uniform at deposition potentials of -600 mV versus Ag/AgCl. The bandgap energy and type of optical transition were determined from optical absorbance data. The film was found to exhibit direct transition in the visible spectrum with a bandgap value of about 1.58 eV.

Key words: Electrodeposition, Cyclic voltammetry, Thin films, Semiconducting material

INTRODUCTION

In search of new semiconducting materials for efficient solar energy conversion through photoelectrochemical solar cells, metal chalcogenides are increasingly studied. The vast preparation and studies of metal chalcogenides thin films can be classified into two categories: binary compounds and ternary compounds. Examples of binary compounds are MnS (Gumus et al., 2005), ZnSe (Riveros et al., 2001), Cu_2S (Anuar et al., 2002), SnSe (Zainal et al., 2003) and SnS (Subramanian et al., 2001) while CuInSe_2 (Pathan and Lokhande, 2005), CdSSe (Mane and Lokhande, 1997) and CuInS_2 (Berenguier and Lewerenz, 2005) are examples of ternary metal chalcogenides. For photovoltaic cells, ternary systems of the compound semiconductors are particularly interesting. Among the ternary semiconducting materi-

als, sulphur-containing compounds occupy an important place. There are many methods for preparing thin films such as chemical bath deposition (Cortes et al., 2004), electrodeposition (Mahalingam et al., 1999), thermal evaporation (Lee et al., 1999), spray pyrolysis (Nascu et al., 1997), sputter deposition (Gupta et al., 2006) and plasma-enhanced chemical vapor deposition (Atif et al., 2006). Amongst these deposition methods, electrodeposition is more attractive, since it offers the advantages of simplicity, economy and convenience and several experimental parameters can be controlled more precisely.

In this paper, we studied the voltammetric behavior of the copper tin sulfide on indium tin oxide glass substrate from aqueous solutions. The thin films were prepared by electrodeposition at different deposition potentials. We investigated the influence of the deposition potential on the optical properties, morphological and structural characteristics of electrodeposited thin films by using UV-Visible spectrophotometer, atomic force microscopy and X-ray diffraction, respectively.

MATERIALS AND METHODS

The deposition bath contained copper sulfate (CuSO_4), tin chloride ($\text{SnCl}_2 \cdot 2\text{H}_2\text{O}$) and sodium thiosulfate ($\text{Na}_2\text{S}_2\text{O}_3 \cdot 5\text{H}_2\text{O}$). All the reagents used were of analytical grade. The pH of the solution was adjusted to 1 by using HCl. The pH was maintained low to prevent the formation of hydroxyl and insoluble compounds. Films were deposited using a three-electrode cell. The Bioanalytical System BAS 100W electrochemical analyzer was employed for recording the cyclic voltammograms and controlling the deposition potentials. The electrodes were an indium-doped tin oxide (ITO) glass substrate as the working electrode, a platinum wire as the counter electrode and a silver-silver chloride as the reference electrode. The substrates were cleaned ultrasonically in water and ethanol before use. Purified nitrogen was flowed into the deposition bath for a few minutes to create oxygen-free environment. The experiment was carried out at room temperature. In order to determine the optimum condition, the films were deposited at various deposition potentials, ranging from -400 mV to -1000 mV versus Ag/AgCl. Upon deposition, the deposits were rinsed with distilled water and kept for further analysis.

X-ray diffraction (XRD) analysis was carried out, using a Philips PM 11730 diffractometer for the 2θ ranging from 30° to 60° with $\text{CuK}\alpha$ ($\lambda=1.5418$ Å) radiation. Topography was measured by using an atomic force microscopy (Quesant Instrument Corporation, Q-Scope 250) operating in contact mode, with a commercial Si_3N_4 cantilever. Optical absorption study was carried out, using the Perkin Elmer UV/Vis Lambda 20 spectrophotometer. The film-coated ITO glass was placed across the sample radiation pathway while the uncoated ITO glass was put across the reference path. The absorption data were manipulated for the determination of the band gap energy, E_g .

RESULTS AND DISCUSSIONS

Cyclic voltammetry

Cyclic voltammetry was used to monitor the electrochemical reactions in solutions of CuSO_4 , $\text{SnCl}_2 \cdot 2\text{H}_2\text{O}$ and $\text{Na}_2\text{S}_2\text{O}_3 \cdot 5\text{H}_2\text{O}$, then in their combined solution of the same concentration and pH (Figure 1). The cyclic voltammogram was scanned in the potential range 1000 mV to -1000 mV versus Ag/AgCl at a sweep rate 10 mVs^{-1} . All voltammetry curves were scanned first in the cathodic direction and positive current indicated a cathodic current.

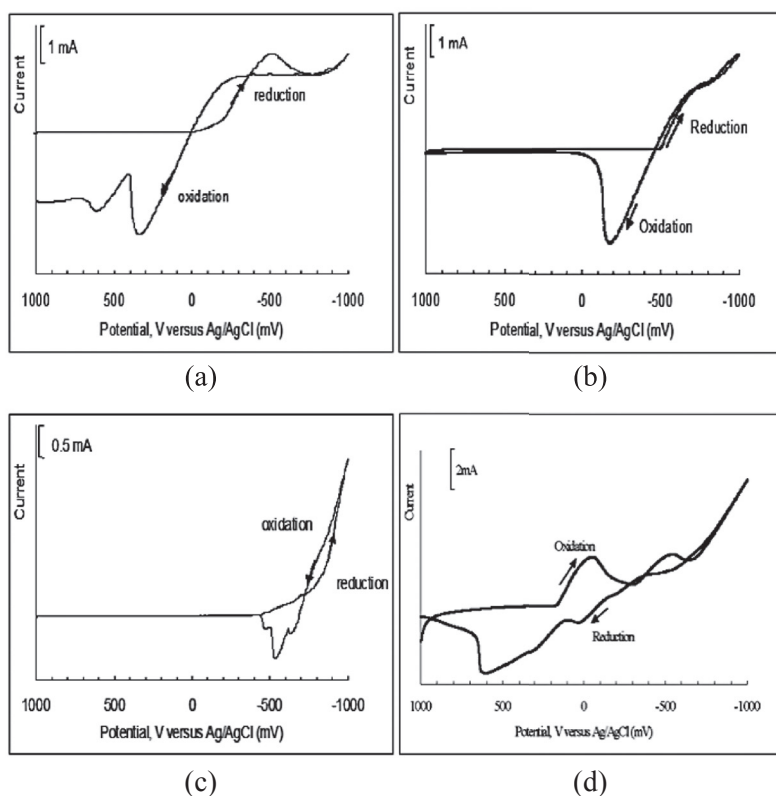


Figure 1: Cyclic voltammogram or (a) 0.01 M copper sulfate (b) 0.01M tin chloride (c) 0.01M sodium thiosulfate (d) mixture of (a), (b) and (c) solutions at room temperature, scan rate: 10 mV/s and pH 1.

In the case of copper sulfate solution (Figure 1a), the current rise started at -50 mV, followed by large reduction wave at -500 mV. This response was associated with Cu (II) reduction on ITO substrate. The deposition reaction was reconfirmed by the reverse scan. The two stripping peaks at positive potential limits, 200-600 mV indicated the oxidation of the copper compound.

Figure 1b shows the voltammogram recorded for tin chloride on ITO glass substrate. The forward scan showed a reduction potential starting at about -500 mV. This was due to the reduction process of tin onto the working electrode. The

reduction peak increased towards the more-negative region where hydrogen evolution also occurred. During the reverse scan, the oxidation wave of tin could be seen starting at about -450 mV. This peak reached a maximum value of about -200 mV. This oxidation peak clearly showed that the process was reversible whereby the deposited tin dissolved upon reversing the potential.

The forward scan of sodium thiosulfate solution (Figure 1c) shows the cathodic current to start flowing at about -500 mV. The shoulder at -700 mV might be associated with the reduction of thiosulphate ions. This reduction wave could be due to the $S_2O_3^{2-}$ ions released during the disproportionation of $Na_2S_2O_3$ at the pH of 1.0.

Figure 1d shows the cyclic voltammogram of the ITO working electrode in the mixture of copper sulfate, tin chloride and sodium thiosulfate. The wave around -475 mV corresponded to the formation of Cu_4SnS_4 layers and the cathodic current increased gradually up to -1000 mV, indicating the growth of layers. The anodic peak around 54 mV corresponded to the stripping of deposited layers in the reverse scan. Based on the above results, the voltammogram suggested that a deposition on the working electrode can be expected when the potentials above -500 mV are applied.

XRD analysis

Figure 2 shows the XRD pattern for the films deposited at various deposition potentials ranging from -400 mV to -1000 mV. Four main peaks at $2\theta = 30.3^\circ$, 35.5° , 45.2° and 50.6° , corresponding to d-spacing values 2.95, 2.55, 2.00 and 1.80 Å which attributed to the (221), (420), (512) and (711) planes, respectively were detected from all the samples. All these peaks are related to the compound of Cu_4SnS_4 of orthorhombic structure ($a = 13.5580$ Å, $b = 7.6810$ Å, $c = 6.4120$ Å, $\alpha = \beta = \gamma = 90^\circ$) (Jaulmes *et al.*, 1977). Since not many researches have been done for these compounds from other methods such as chemical bath deposition, evaporation deposition, comparison of data could not be concluded at the moment. However, these observed d spacing values and the standard values were in good agreement with the Joint Committee on Powder Diffraction Standards values (Reference code: 010710129) in Table 1 that showed the highest peak at 2.95 Å, corresponding to (221) plane. Raising the deposition potential further to -600 mV and more negative of values, resulted in the disappearance of the plane (022) and some new peaks gradually could be observed. The new peaks corresponded to copper sulfide (Reference code: 000653556) that started to appear at -700 mV, while peaks for sulfur (Reference code: 010740791) could be observed at above -900 mV.

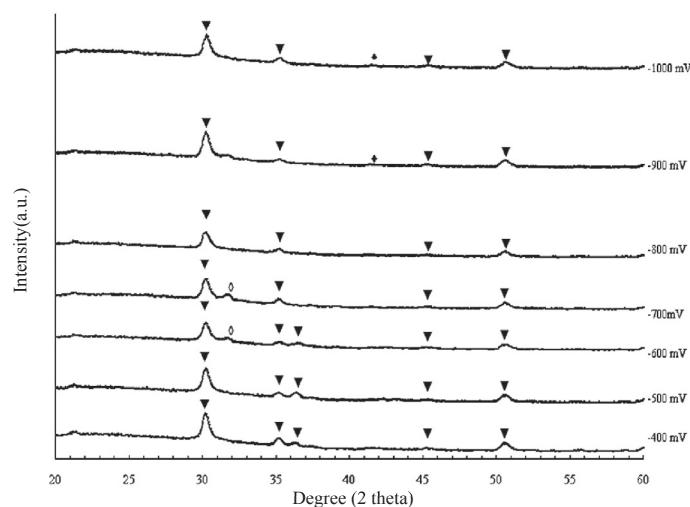


Figure 2: X-ray diffraction pattern of samples prepared at different deposition potentials Cu_4SnS_4 (▼) S_{12} (◆) CuS (◇).

AFM analysis

In order to achieve a more direct insight into the surface structural features of the films, atomic force microscopy (AFM) imaging had been performed. The surface images in an area of $10\ \mu\text{m} \times 10\ \mu\text{m}$ of the thin films deposited at various deposition potential values are shown in Figure 3. It can be observed that the surface of the films was not very compact (Figure 3a). The films were constituted by nano particles with an irregular size distribution. A lot of empty spaces could be seen between these particles.

AFM images of samples clearly show the conversion of nano particles into spherical grains that were quite uniform over the entire glass substrate (Figure 3c). However, it is seen from the intensity distribution that the film consisted of smaller and larger nano particles in deposition potential above $-700\ \text{mV}$ (Figure 3d-g). This might be due to the difference of rate of nucleation and growth. At the right hand side of the image, intensity strip is shown which indicates the height of the surface grain along Z-axis. AFM picture shows the presence of high hills on top of a homogeneous granular background surface. The height of the hills was found to be decreased as the deposition potential increased.

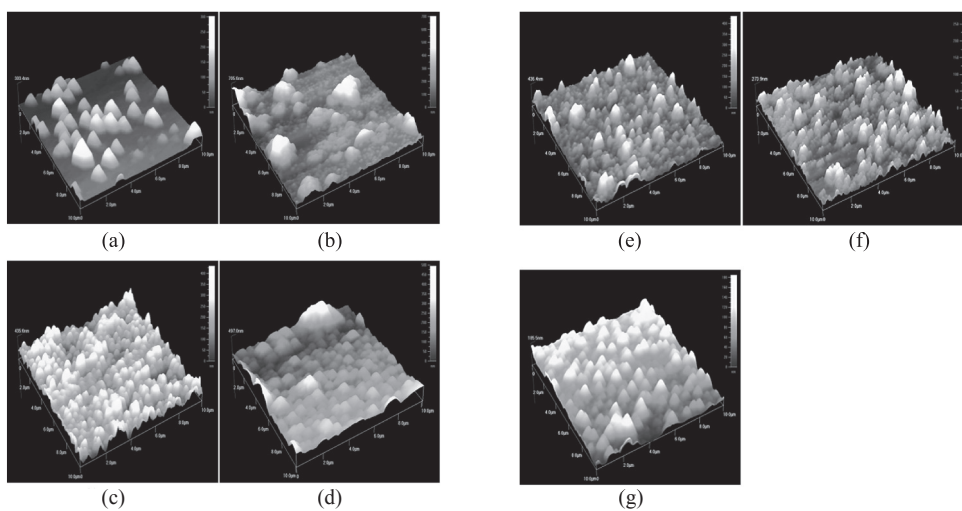


Figure 3: Atomic force microscopy images of Cu_4SnS_4 thin films at different deposition potentials (versus Ag/AgCl)
 (a) -400 mV (b) -500 mV (c) -600 mV (d) -700 mV (e) -800 mV
 (f) -900 mV (g) -1000 mV.

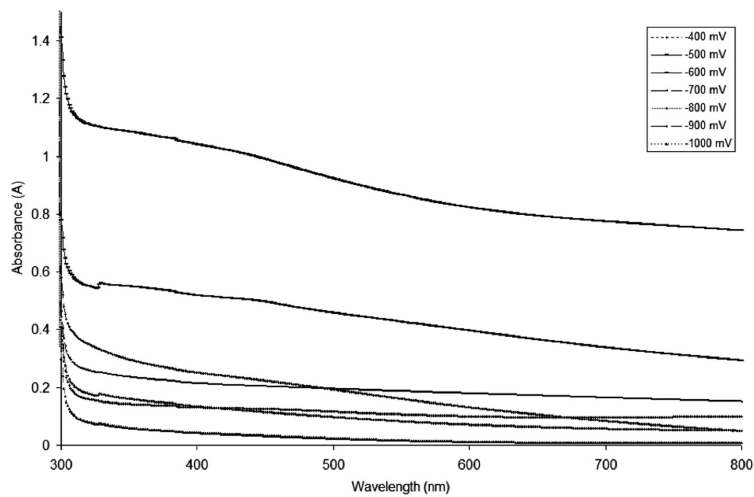


Figure 4: Absorbance versus wavelength spectra for Cu_4SnS_4 films deposited at different deposition potentials (versus Ag/AgCl)

Table 1. Comparison between observed d spacing values of Cu₄SnS₄ at different deposition potential with JCPDS data.

Deposition	2θ (°)	d-spacing		Compounds
		Observed values (Å)	JCPDS data (Å)	
-400 mV	30.2	2.96	2.96	Cu ₄ SnS ₄
	35.2	2.55	2.54	Cu ₄ SnS ₄
	36.4	2.47	2.46	Cu ₄ SnS ₄
	45.2	2.01	2.00	Cu ₄ SnS ₄
	50.5	1.81	1.80	Cu ₄ SnS ₄
-500 mV	30.3	2.95	2.96	Cu ₄ SnS ₄
	35.2	2.55	2.54	Cu ₄ SnS ₄
	36.4	2.47	2.46	Cu ₄ SnS ₄
	45.3	2.00	2.00	Cu ₄ SnS ₄
	50.6	1.80	1.80	Cu ₄ SnS ₄
-600 mV	30.2	2.96	2.96	Cu ₄ SnS ₄
	31.7	2.82	2.82	CuS
	35.2	2.55	2.54	Cu ₄ SnS ₄
	36.5	2.46	2.46	Cu ₄ SnS ₄
	45.2	2.00	2.00	Cu ₄ SnS ₄
	50.6	1.80	1.80	Cu ₄ SnS ₄
-700 mV	30.3	2.95	2.96	CuS
	31.7	2.82	2.82	Cu ₄ SnS ₄
	35.1	2.56	2.54	Cu ₄ SnS ₄
	45.2	2.00	2.00	Cu ₄ SnS ₄
	50.6	1.80	1.80	Cu ₄ SnS ₄
-800 mV	30.2	2.96	2.96	Cu ₄ SnS ₄
	35.2	2.55	2.54	Cu ₄ SnS ₄
	45.3	2.00	2.00	Cu ₄ SnS ₄
	50.6	1.80	1.80	Cu ₄ SnS ₄
-900 mV	30.2	2.96	2.96	Cu ₄ SnS ₄
	35.3	2.55	2.54	Cu ₄ SnS ₄
	41.4	2.18	2.17	S ₁₂
	45.2	2.01	2.00	Cu ₄ SnS ₄
	50.6	1.80	1.80	Cu ₄ SnS ₄
-1000 mV	30.3	2.95	2.96	Cu ₄ SnS ₄
	35.3	2.54	2.54	Cu ₄ SnS ₄
	41.6	2.17	2.17	S ₁₂
	45.4	2.00	2.00	Cu ₄ SnS ₄
	50.6	1.80	1.80	Cu ₄ SnS ₄

Optical properties

Deposition was carried out on an ITO glass substrate to study the optical behavior of the Cu_4SnS_4 films. Figure 4 shows the optical absorbance data of the films versus wavelength obtained from UV-Visible spectrophotometer. The absorption could be observed between 300 to 700 nm. The spectrum shows a gradually increasing absorbance throughout the visible region for all samples, which makes it possible for this material to be used in a photoelectrochemical cells. The absorbance of thin films deposited at -600 mV produced higher absorbance value. However, it is seen from figure that as the deposition potential increased (above -700 mV), the absorbance value decreased.

The band gap energy and transition type was derived from mathematical treatment of data obtained from optical absorbance versus wavelength with the following relationship for near-edge absorption (Zainal *et al.*, 2004):

$$A = \frac{[k(h\nu - E_g)^{n/2}]}{h\nu} \quad (1)$$

where ν is the frequency, h is the Planck's constant, k equals to constant while n carries the value of either 1 or 4. The value of n is 1 and 4 for the direct transition and indirect transition, respectively. The band gap, E_g , could be obtained from a straight line plot of $(Ah\nu)^{2/n}$ as a function of $h\nu$. Extrapolation of the line to the base line, where the value of $(Ah\nu)^{2/n}$ is zero, will give E_g . The straight-line plot in Figure 5a indicates that the energy band gap of Cu_4SnS_4 is direct transition and yields a band gap of 1.58eV. Further analysis on Figure 5b, as a comparison plot for indirect transition ($n=4$), showed negative band gap value that is inappropriate and unacceptable even though correlation coefficient (R^2) for straight line fit of 0.9993.

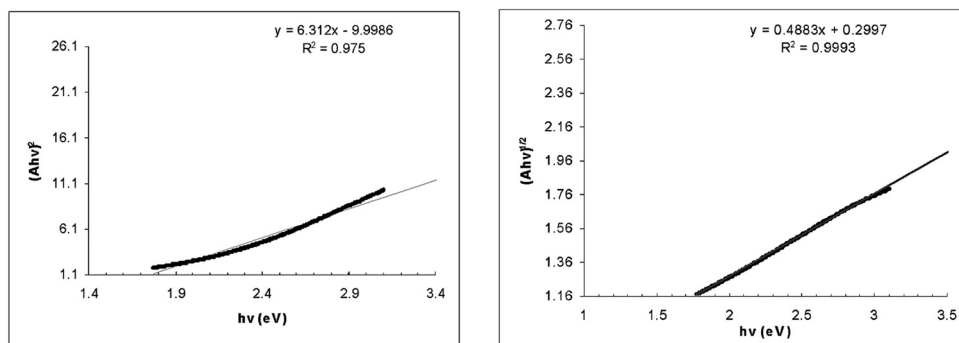


Figure 5: Plot of $(Ah\nu)^{2/n}$ versus $h\nu$ for deposited thin films at -0.6 V (a) $n=1$ for direct transition (b) $n=4$ for indirect transition

Table 2 lists the direct band gap for the Cu_4SnS_4 thin films deposited at different deposition potentials. The direct band gap energy of the thin films initially increased (1.61 to 1.65 eV) with increasing the cathodic potential from -400 mV to -500 mV . The films had direct energy band gap of 1.58 eV, close to optimum value required for efficient light absorption at -600 mV . However, further increasing in deposition potential (more negative than -700 mV) caused increasing in the band gap energy. Therefore, the deposition potential has some influence on the band gap of the films.

Table 2. The direct band gap energy for the Cu_4SnS_4 films deposited at different deposition potentials

Deposition potential (versus Ag/AgCl)	Direct transition (eV)
-400 mV	1.61
-500 mV	1.65
-600 mV	1.58
-700 mV	1.60
-800 mV	1.84
-900 mV	1.86
-1000 mV	1.97

CONCLUSION

Cu_4SnS_4 thin films cathodically electrodeposited on an indium tin oxide glass substrate were found to be of orthorhombic structure as indicated by their XRD patterns. Decreasing in deposition potential resulted in an increase in the size of the grains and caused in growth of spherical particles. The film was found to exhibit direct transition in the visible spectrum with a bandgap value of about 1.58 eV at -600 mV . The film deposited at -600 mV showed the best optimum condition for preparation of Cu_4SnS_4 films because of higher absorption characteristics when compared to the film prepared at other deposition potentials. This result correlates well with the information obtained from the XRD and AFM which shows good film formation at this potential.

ACKNOWLEDGEMENTS

The authors would like to thank the Department of Chemistry, Universiti Putra Malaysia for the provision of laboratory facilities.

REFERENCES

- Anuar, K., Z. Zainal, M.Z. Hussein, N. Saravanan, and I. Haslina. 2002. Cathodic electrodeposition of Cu_2S thin film for solar energy conversion. *Solar Energy Materials & Solar Cells* 73: 351-356.
- Atif, M.A., I. Takao, and H. Seiichi. 2006. Structural and photo-luminescence

- properties of nanocrystalline silicon films deposited at low temperature by plasma-enhanced chemical vapor deposition. *Applied Surface Science* 253: 1198-1204.
- Berenguier, B., and H.J. Lewerenz. 2005. Efficient solar energy conversion with electrochemically conditioned CuInS_2 thin film absorber layers. *Electrochemistry Communications* 8: 165-169.
- Cortes, A., H. Gomez, R.E. Marotti, G. Riveros, and E.A. Dalchiele. 2004. Grain size dependence of the bandgap in chemical bath deposited CdS thin films. *Solar Energy Materials & Solar Cells* 82: 21-34.
- Gumus, C., C. Ulutas, R. Esen, O.M. Ozkendir, and Y. Ufuktepe. 2005. Preparation and characterization of crystalline MnS thin films by chemical bath deposition. *Thin Solid Films* 492: 1-5.
- Gupta, A., V. Parikh, and A.D. Compaan. 2006. High efficiency ultra-thin sputtered CdTe solar cells. *Solar Energy Materials and Solar Cells* 90(15): 2263-2271
- Jaulmes, S., J. Rivet and P. Laruelle. 1977. Copper tin sulfide (Cu_4SnS_4). *Acta Crystallographica Section B*: 540-542.
- Lee, Y.H., W.J. Lee, Y.S. Kwon, G.Y. Yeom, and J.K. Yoon. 1999. Effects of CdS substrates on the physical properties of polycrystalline CdTe films. *Thin Solid Films* 341 (1-2): 172-175.
- Mahalingam, T., B. Subramanian, C. Sanjeeviraja, M. Jayachandran, and J.C. Mary. 1999. Electrodeposition of Sn, Se, SnSe and the material properties of SnSe films. *Thin Solid Films* 357: 119-124.
- Mane, R.S., and C.D. Lokhande. 1997. Studies on chemically deposited cadmium sulphoselenide (CdSSe) films. *Thin Solid Films* 304: 56-60.
- Nascu, C., I. Pop, V. Ionescu, E. Indrea, and I. Bratu. 1997. Spray pyrolysis deposition of CuS thin films. *Materials Letters* 32: 73-77.
- Pathan, H.M., and C.D. Lokhande. 2005. Chemical deposition and characterization of copper indium diselenide (CISE) thin films. *Applied Surface Science* 245: 328-334.
- Riveros, G., H. Gomez, R. Henriquez, R. Schrebler, R.E. Marotti, and E.A. Dalchiele. 2001. Electrodeposition and characterization of ZnSe semiconductor thin films. *Solar Energy Materials & Solar Cells* 70: 255-268.
- Subramanian, B., C. Sanjeeviraja, and M. Jayachandran. 2001. Cathodic electrodeposition and analysis of SnS films for photoelectrochemical cells. *Materials Chemistry and Physics* 71: 40-46.
- Zainal, Z., J.A. Ali, K. Anuar, and M.Z. Hussein. 2003. Electrodeposition of tin selenide thin film semiconductor: effect of the electrolytes concentration on the film properties. *Solar Energy Materials & Solar Cells* 79: 125-132.
- Zainal, Z., Saravanan, N., Anuar., M.Z. Hussein, and W.M.M. Yunus. 2004. Chemical bath deposition of tin selenide thin films. *Materials science and Engineering B* 107: 181-185.